

1 **Comprehensive bioinformatic analysis of newly sequenced *Turdoides affinis***  
2 **mitogenome reveals the persistence of translational efficiency and dominance of NADH**  
3 **dehydrogenase complex-I in electron transport system over Leiothrichidae family**

4 Indrani Sarkar, PrateekDey, Sanjeev Kumar Sharma, Swapna Devi Ray, Ram Pratap Singh\*

5 National Avian Forensic Laboratory, Sálim Ali Centre for Ornithology and Natural History,

6 Anaikatty, Coimbatore – 641108, Tamil Nadu, India

7

8

9

10

11 **Running title:** Mitogenome of yellow-billed babbler

12

13

14

15 **\*Corresponding Author:**

16 Dr. Ram Pratap Singh, Senior Scientist

17 Sálim Ali Centre for Ornithology and Natural History, Anaikatty

18 Coimbatore – 641 108, Tamil Nadu, India

19 Ph. +91-422-2203136

20 Email: [rampratapsingh81@gmail.com](mailto:rampratapsingh81@gmail.com)

21

22 **Abstract**

23 Mitochondrial genome provides useful information about species with respect to its evolution  
24 and phylogenetics. We have taken the advantage of high throughput next-generation  
25 sequencing technique to sequence the complete mitogenome of Yellow-billed babbler  
26 (*Turdoides affinis*), a species endemic to Peninsular India and Sri Lanka. Both, reference-  
27 based and *de-novo* assemblies of mitogenome were performed and observed that *de-novo*  
28 assembled mitogenome was most appropriate. The complete mitogenome of yellow-billed  
29 babbler (assembled *de-novo*) was 17,671 bp in length with 53.2% AT composition. Thirteen  
30 protein-coding genes along with 2 rRNAs and 22 tRNAs were detected along with duplicated  
31 control regions. The arrangement pattern of these genes was found conserved among  
32 Leiothrichidae family mitogenomes. Downstream bioinformatics analysis revealed the effect  
33 of translational efficiency and purifying selection pressure over all the thirteen protein-coding  
34 genes in yellow-billed babbler mitogenome. Moreover, genetic distance and variation  
35 analysis indicated the dominance of NADH dehydrogenase complex-I in the electron  
36 transport system of *T. affinis*. Evolutionary analysis revealed the conserved nature of all the  
37 protein-coding genes across Leiothrichidae family mitogenomes. Our limited phylogenetics  
38 results suggest that *T. affinis* is closer to *Garrulax*.

39 **Key Words:** Phylogeny, mitochondrial DNA, birds, tRNA, Control region

40

## 41 **Introduction**

42 Aves are one of the most diverse vertebrate classes with a huge number of species having a  
43 broad range of ecological behavior and complex morphology, all of which make it difficult to  
44 solve the riddles regarding their taxonomy along with phylogenetic and evolutionary  
45 relationship<sup>1-3</sup>. New and advanced scientific techniques have emerged to solve these riddles.  
46 For the last few years, genome sequencing has become more popular to obtain huge  
47 information on evolutionary history and revising the clustering pattern of traditional  
48 taxonomy<sup>4</sup>. Mitochondrial DNA with some of its inherent properties like small genome size,  
49 absence of extensive recombination frequency, simple structure of genome, maternal  
50 inheritance along with rapid evolutionary rate are now extensively utilized in taxonomic and  
51 phylogenetic studies of vertebrates<sup>5-10</sup>. Furthermore, it has been reported that, complete  
52 mitogenomes retain more information than a single gene regarding the evolutionary history  
53 of the taxon and also provide consistent results compared to nuclear genes<sup>11</sup>. This also  
54 reduces the effect of homoplasy and frequent stochastic errors in phylogenetic studies<sup>11</sup>.

55 Yellow-billed bababler (*Turdoides affinis*) is one of the most common birds in India<sup>12</sup>. They  
56 are distributed in the southern peninsular India including the southern part of Maharashtra,  
57 Chattisgarh and Andhra Pradesh<sup>12</sup>. The taxonomic classification of this bird is quite dubious.  
58 Previously all babbler and allies were considered under Timaliidae family<sup>13</sup>. Recent  
59 classification studies have split this family into five discrete families<sup>13</sup>. Three of them,  
60 Leiothrichidae, Pellorneidae and Timaliidae consisted of traditional babblers while  
61 Zosteropidae included mainly *Yuhina* along with some other minor species and Sylviidae  
62 grouped all the *Sylvia warblers*<sup>14</sup>. Among these five distinct families, Leiothrichidae  
63 represented the largest group consisting of 125 species distributed mainly in the Sino-  
64 Himalayan and South-Eastern parts of Asia<sup>14</sup>. A study on the Leiothrichidae family suggested  
65 their origin prior to the Miocene–Pliocene boundary, which is well known for its noteworthy

66 climatic turmoil in Asia<sup>13</sup>. Hence, it is imperative to conduct in-depth molecular studies on  
67 this family to know some very appealing unknown facts regarding their taxonomical and  
68 phylogenetic relationships.

69 This Leiothrichidae family mainly consisted of *Grammatoptila*, *Garrulax*, *Trochalopteron*,  
70 *Turdoides* and *Argya*<sup>14</sup>. Polyphyletic nature was observed among members of *Turdoides* due  
71 to which further taxonomic classification was done and some species were resurrected from  
72 this genus<sup>14-16</sup>. Yellow-billed babbler which is considered to be under *Turdoides* has been  
73 recently proposed to be under *Argya* based on revised taxonomy of Leiothrichidae<sup>14</sup>;  
74 however, more investigations are required to confirm this. Yellow-billed babbler generally  
75 live in flocks of seven to ten members continuously squeaking, chattering and chirping.  
76 Helpers are seen generally assisting parents in nest building, chick feeding and maintaining  
77 nest sanitation as a cooperative breeding character<sup>17-19</sup>. Interestingly, the close relatives of *T.*  
78 *affinis* for instance, *Garrulax*, *Leiothrix*, *Liocichla*, *Minla* and *Trochalopteron* have still not  
79 been reported to show the cooperative breeding behaviour indicating a divergence of *T.*  
80 *affinis* at least from the behavioural ecology perspective<sup>18</sup>.

81 Untill now, the complete mitogenomes of various species (including *Garrulax affinis*<sup>20</sup>, *G.*  
82 *albogularis*, *G. canorus*, *G. canorus* voucher AHNU, *G. cineraceus*<sup>21</sup>, *G. elliotii*<sup>22</sup>, *G.*  
83 *formosus*<sup>23</sup>, *G. ocellatus*<sup>24</sup>, *G. perspicillatus*<sup>25</sup>, *G. poecilorhynchus* voucher B33<sup>26</sup>, *G.*  
84 *sannio*<sup>27</sup>, *G. sannio* voucher GSAN20150704V3, *Trochalopter onmilnei*, *Leiothrix*  
85 *argentaureis*, *L. lutea*, *Liocichla omeiensis*<sup>28</sup> and *Minla ignotincta*<sup>29</sup>) from Leiothrichidae  
86 family have been reported. However, complete mitogenome of birds representing the genus  
87 *Turdoides* is yet to be revealed.

88 In this study, we have sequenced and described the complete mitochondrial genome of  
89 *T.affinis* obtained using two approaches such as reference-based assembly and *de-novo*  
90 assembly<sup>30-31</sup>. We employed two different genome assembly approaches to align the same

91 mitogenome to quantify the differences occurring due to the alignment approach and their  
92 effect on mitogenomic parameters. In addition, we have performed a detailed comparative  
93 analysis on available mitogenomes of the family Leiothrichidae to understand the overall  
94 species-specific differences including some potent parameters such as codon usage and  
95 evolutionary history.

## 96 **Materials and Methods**

### 97 **Sample collection and DNA extraction**

98 A fresh road-killed specimen of *T. affinis* was collected from Anaikatty Hills in Coimbatore  
99 district of Tamil Nadu, India (Fig. 1), and transported immediately to the lab. Prior  
100 permission for roadkill collection was obtained from Tamil Nadu Forest Department  
101 (Ref.No.WL5 (A)/2219/2018; Permit No. 14/2018). Muscle tissue was sampled from the  
102 specimen and stored in DESS buffer (20% DMSO, 0.25M tetra-sodium EDTA, Sodium  
103 Chloride till saturation, pH 7.5) at -20°C for further processes. About 50 milligram of the  
104 muscle tissue in DESS buffer was taken and added to 500 µl of lysis buffer (10 mM Tris-pH  
105 8.0, 10 mM EDTA-pH 8.0, 100 mM NaCl) and homogenized thoroughly. To the  
106 homogenate, 80 µl of 10% SDS and along with 20 µl of Proteinase K (20 mg/ml) was added  
107 and incubated overnight at 55°C. The DNA extraction was performed the following day  
108 using suitable volumes of Phenol, Chloroform and Isoamyl alcohol. The DNA pellet obtained  
109 was suspended in 100 µl of Tris-EDTA buffer (Sigma-Aldrich, USA) and quantified using  
110 spectrophotometer (DeNovix, USA) and Qubit 4 Fluorometer (ThermoFisher Scientific,  
111 USA). The quality of the DNA extracted was assessed by running it on 1% agarose gel  
112 stained with ethidium bromide intercalating dye.

### 113 **Library preparation**

114 For library preparation, 700 nanograms of extracted DNA was utilized as starting material in  
115 NEBNext Ultra II DNA Library Prep kit for Illumina (New England Biolabs, USA). The  
116 DNA was fragmented using focused ultrasonicator (Covaris M220, USA) until the desired  
117 length of 270-300 base pairs was obtained. The fragmented DNA size was analyzed by  
118 running it in Fragment Analyzer (Agilent, USA) making sure that the size of the majority of  
119 DNA fragments is between 270-300 base pairs. Adaptor ligation was then carried out in a  
120 thermocycler following the “NEBNext Ultra II DNA Library Prep kit for Illumina” protocol  
121 using dual indexed primers present in the kit for creation of pair end libraries. After the  
122 ligation reaction was completed, the size selection of Adaptor-ligated DNA was carried out  
123 using NEBNext Sample Purification Beads (New England Biolabs, USA) followed by PCR  
124 enrichment of Adaptor-ligated DNA following the manufacturer’s protocol. After the clean-  
125 up of the enriched DNA, it was again analysed for the required concentration and mean peak  
126 size in a Fragment Analyzer (Agilent, USA). The enriched DNA library fragments were  
127 subjected to sequencing in Illumina NextSeq 550 (Illumina, Inc., USA) using Illumina High  
128 Output Kit for NextSeq 500/550 (Illumina, Inc., USA). A PhiX control library (Illumina,  
129 Inc., USA) was also subjected to sequencing along with the sample DNA library as an  
130 internal control. At the end of the sequencing run, high quality paired end reads were  
131 obtained, and further bioinformatics analysis was performed.

### 132 **Assembly and annotation of the mitochondrial genome**

133 IlluminaNextSeq 550 produced 88,52,137 raw reads from whole-genome library. Cutadapt  
134 tool<sup>32</sup> was used to trim the adapter and lowquality reads with a Phred (Q) score of 30 was  
135 selected for further analysis. Finally we got 12,97,736 high quality reads after down sampling  
136 with Seqtk (<https://github.com/lh3/seqtk>) which were used for assembly. *De novo* assembly  
137 was performed using SPAdes-3.11.1 software with default parameters. MITOS online server  
138 (<http://mitos.bioinf.uni-leipzig.de/index.py>) was used for annotation of the mitogenome.  
139 Reference-based assembly was also performed as described in supplementary file 1.

## 140 **Phylogenetic analysis**

141 Phylogenetic analysis was performed on the available whole mitogenomes of various species  
142 of the Leiothrichidae family. We prepared two complete mitogenome based phylogenetic  
143 trees, one with *T. affinis* mitogenome assembled through reference-based assembly and  
144 another with *de-novo* assembly using Maximum likelihood algorithm with 1000 bootstrap  
145 values in ClustalW implemented with Mega ver. 7.

## 146 **Sequence analysis of mitogenome**

147 The complete mitogenome of *T. affinis* was compared with other Leiothrichidae family avian  
148 species whose complete mitochondrial genomes are available at NCBI including *Garrulax*  
149 *affinis*<sup>20</sup>, *G. albogularis*, *G. canorus*, *G. canorus* voucher AHNU, *G. cineraceus*<sup>21</sup>, *G.*  
150 *elliottii*<sup>22</sup>, *G. formosus*<sup>23</sup>, *G. ocellatus*<sup>24</sup>, *G. perspicillatus*<sup>25</sup>, *G. poecilorhynchus* voucher  
151 B33<sup>26</sup>, *G. sannio*<sup>27</sup>, *G. sannio* voucher GSAN20150704V3, *Trochalopteron milnei*, *Leiothrix*  
152 *argentauris*, *L. lutea*, *Liocichla omeiensis*<sup>28</sup> and *Minla ignotineta*<sup>29</sup>. These sequences were  
153 downloaded from NCBI website and used for further comparative analysis. The protein-  
154 coding genes along with tRNAs and rRNAs were aligned to examine whether any  
155 rearrangements persist among these mitogenomes. The initial and terminating codons of all  
156 the protein-coding genes were curated through NCBI ORF finder  
157 (<https://www.ncbi.nlm.nih.gov/orffinder/>). Circular genome views were obtained by CG view  
158 server<sup>33</sup>. The boundary of the control region (CR) was determined<sup>34</sup>.  
159 Detailed codon usage analysis of the select mitogenomes was performed using  
160 CodonWsoftware<sup>35</sup>. The studied codon usage parameters include Relative Synonymous  
161 codon Usage (RSCU), Effective number of Codons (ENc) and frequency of G+C at the third  
162 position of codons (GC3s). Different codon composition indices of individual genes, for  
163 example total GC content as well as the frequency of each nucleotide at the third position of  
164 codons (A3, T3, G3 and C3) were also estimated. R-based heatmaps were generated based on

165 the overall codon usage and amino acid usage analysis. Skew values for AT[(A-T)/(A+T)]  
166 and GC [(G-C)/(G+C)] were calculated<sup>36</sup> using DAMBE software  
167 (<http://dambe.bio.uottawa.ca/DAMBE/dambe.aspx>). Tandem Repeats Finder software  
168 (<https://tandem.bu.edu/trf/trf.html>) with its default settings was employed to detect any  
169 tandem repeats within the mitogenomes. A BlastN based approach to find intra-genomic  
170 duplication of large fragments or interspersed repeats was employed<sup>37</sup>, where each  
171 mitogenome was searched against itself with an e-value of 1e-10. This analysis detected a  
172 negligible number of interspersed repeats, hence was not evaluated further.

### 173 **Estimation of translational efficiency**

174 This parameter measures the competence of codon-anticodon interactions indicating the  
175 accuracy of the translational machinery of genes in the absence of preferred codon set  
176 information. We calculated the translational efficiency according to the following equation<sup>38</sup>:

$$P2 = \frac{WWC + SSU}{WWY + SSY}$$

177 where, W= A or U, S=C or G and Y=C or U.

178  $P2 > 0.5$  indicates the existence of translational selection.

### 179 **RSCU based cluster analysis and putative optimal codons**

180 Generally, highly expressed genes utilize a specific set of codons termed as optimal codons.  
181 Due to the preferential use of this set of codons their Enc value lowers down in contrast to  
182 lowly expressed genes, which restrain more rare codons with higher Encvalue<sup>35</sup>. We  
183 identified the optimal codons of all investigated species from their RSCU values. RSCU =1  
184 indicated unbiased codon usage whereas; RSCU > 1 and RSCU < 1 indicated a higher and  
185 lower usage frequency of that particular codon respectively<sup>35</sup>.

### 186 **Evolutionary analysis**



187 The ratio ( $\omega$ ) of non-synonymous substitution rate per synonymous site ( $k_a$ ) to synonymous  
188 substitution rate per non-synonymous site ( $k_s$ ) has been reported to be an excellent estimator  
189 of evolutionary selection pressure or constrain on protein-coding genes.  $\omega > 1$  stands for  
190 positive Darwinian selection (diversifying pressure), on the contrary,  $\omega < 1$  signifies purifying  
191 or refining selection. At neutral evolutionary state, the value of  $\omega$  becomes 1 symbolizing the  
192 equal rate of both synonymous and non-synonymous substitution<sup>39</sup>. The mean genetic  
193 distance of the annotated protein-coding genes of the studied mitogenomes were calculated in  
194 terms of Kimura-2-parameter (K2P) substitution model and evolutionary rate ( $\omega$ ) was  
195 calculated by DnaSPver 6.12.03 software<sup>40</sup>.

## 196 **Results and Discussion**

### 197 **Comparison of *T. affinis* mitogenome assembled using reference-based and *de-novo*** 198 **assembly approach**

199 In this study, we performed both, reference-based assembly and *de-novo* assembly of the  
200 newly sequenced mitogenome of *T. affinis* and found a considerable difference in the results  
201 between these two approaches. In reference-based assembly, the total size of the mitogenome  
202 was 16,861 bp with 47% GC and 53% AT (Supplementary file 1) whereas the *de-*  
203 *novo* assembly resulted in 17,671 bp long mitogenome with 53.2% AT and 46.80% GC (Fig.  
204 2, Table 1). AT and GC skewness were 0.13 and -0.38, respectively for *de-novo* assembly.  
205 However, reference-based assembly resulted in lower AT (0.05) and GC skew (-0.14) for *T.*  
206 *affinis* mitogenome. The Genbank accession number of complete *T. affinis* mitogenome  
207 (assembled *de-novo*) is MN848144.

208 Two rRNA (*rrnS* for small subunit and *rrnL* for large subunit), 13 protein-coding genes  
209 (PCGs) and 22 tRNAs specified for 20 amino acids (two tRNAs each for serine and lysine)  
210 were reported in both the mitogenomes. The total length of PCGs, tRNAs and rRNAs were  
211 11244 bp, 1539 bp and 2389 bp, respectively for *de-novo* assembly while these were 11247  
212 bp, 1535 bp and 2578 bp respectively for reference-based assembly.

213 The following results were identical for both the mitogenomes. For instance, most of tRNAs  
214 (16) were distributed on the positive (+) strand except trnQ(CAA), trnA(GCA), trnN(AAC),  
215 trnC(TGC), trnY(TAC) and trnS2(TCA) that were distributed on the negative (-) strand. Both  
216 rRNAs along with all the PCGs, except nad6, were present on the negative (-) strand.

217 Two non-coding control regions were found and referred to as CR1 and CR2. The 5'  
218 boundary of CR1 was trnT(ACA) and 3' boundary was trnP(CCA) while CR2 was present  
219 between trnE(GAA) and trnF(TTC). Length of CR1 and CR2 were 1138 bp and 1159  
220 bp, respectively in *de-novo* assembly (at parwith the other compared species) while for  
221 reference-based assembly CR1 was 825bp (less than the average CR1 length of other  
222 compared species by 300bp) and CR2 was 1539bp long (extra 390bp than the average CR2  
223 length of compared species). The nucleotide composition of both CR1 and CR2 was  
224 calculated. AT of CR1 was 54.63% (45.37% GC) for *de-novo* assembly and 53.68% (46.32%  
225 GC) for reference-based assembly. CR2 showed 53.78% AT (46.22% GC) and 55.9% AT  
226 (44.1% GC) for *de-novo* and reference-based assembly, respectively indicating a bias towards  
227 an AT for these regions. rRNAs, tRNAs and PCGs were arranged in the following manner in  
228 both the assemblies:

229 trnF-rrnS-trnV-rrnL-trnL2-nad1-trnI-trnQ-trnM-nad2-trnW-trnA-trnN-trnC-trnY-cox1-trnS2-  
230 trnD-cox2-trnK-atp8-atp6-cox3-trnG-nad3-trnR-nad4l-nad4-trnH-trnS1-trnL1-nad5-cob-  
231 trnT-trnP-nad6-trnE.

232 These results showed considerable differences between reference-based assembly and *de-*  
233 *novo* assembly. Further, we performed a limited phylogenetic analysis with both the  
234 mitogenomes, and observed that *de-novo* assembled mitogenome performed better. The  
235 phylogenetic analysis of reference-based assembled mitogenome placed  
236 *T. affinis* with *Leiothrix lutea*(Supplementary file 2), whereas in case of *de-novo* assembled  
237 mitogenome based phylogeny, *T. affinis* formed a discrete group which was placed  
238 near *Garrulax affinis*(Fig. 3). The later finding is consistent with a recent report<sup>14</sup> that revised

239 the taxonomy of Leiothrichidae using a set of nuclear genes with a mitochondrial PCG as a  
240 phylogenetic marker. Though our phylogenetic results are limited because of the  
241 unavailability of complete mitogenome sequences of other groups, still it provides supporting  
242 evidences that *de novo* assembled mitogenome is more appropriate.

### 243 **Nucleotide composition and translational efficiency**

244 The newly sequenced complete mitogenome of *T. affinis* was compared with other available  
245 mitogenomes from the Leiothrichidae family (Table 2). We considered *Garrulax*  
246 *affinis*(KT182082.1)<sup>20</sup>, *G. albogularis*(KX082660.1), *G. canorus*(KT633399.1), *G. canorus*  
247 voucher AHNU (JQ348398.1), *G. cineraceus*(KF926988.1)<sup>21</sup>, *G. elliotii*(KT272404.1)<sup>22</sup>, *G.*  
248 *formosus*(KR020504.1)<sup>23</sup>, *G. ocellatus*(KP995195.1)<sup>24</sup>, *G. perspicillatus*(KF997865.1)<sup>25</sup>, *G.*  
249 *poecilorhynchus* voucher B33 (KR909134.1)<sup>26</sup>, *G. sannio*(KR869824.1)<sup>27</sup>, *G. sannio* voucher  
250 GSAN20150704V3 (KT373847.1), *Leiothrix argentauris*(HQ690245.1), *L.*  
251 *lutea*(JQ423933.1), *Liocichla omeiensis*(KU886092.1)<sup>28</sup>, *Minla ignotincta*(KT995474.1)<sup>29</sup>  
252 and *Trochalopteron milnei*(MH238447.1). Gene arrangement pattern was observed among  
253 these species and was found similar to that of *T. affinis* (Fig. 4). Values of AT skew ranged  
254 from 0.09 (*T. milnei*) to 0.13 (*Turdoides affinis*) while the GC skew ranged from -0.39 (*G.*  
255 *albogularis*) to -0.36 (*L. omeiensis*) (Table 2). Comparative RSCU analysis identified a set of  
256 optimal codons common among all species - GCC(A), UGC(C),UUC(F), GGA(G), AAA(K),  
257 CUA(L), UUA(L), AUA(M), CCU(P), CAA(Q), AGC(S), ACC (T) and GUA(V). Along  
258 with these GCU(A), GCA(A), GAC(D), GAA(E), CAC(H), AUU(I), CUC(L), CUU(L),  
259 AAU(N), CCC(P), CGC(R), UCU(S), ACU(T), GUC(V), UGA(W) and UAC(Y) were also  
260 frequently used in *T. affinis*. Heatmaps based on codon and amino acid usage (Fig. 5)  
261 analysis of compared mitochondrial genomes validated the aforementioned codon preference.  
262 GC3 vs. Enc plot analysis has been proved very efficient in predicting whether translational  
263 selection or mutational pressure persist over the genes of interest<sup>35</sup>. The GC3-Enc

264 plots(Fig.6a) of protein-coding genes of the compared mitogenomes were placed well below  
265 the curve indicating the predominance of selection pressure over mutational bias. RSCU  
266 analysis revealed a higher degree of concord among Leiothrichidae mitogenomes from the  
267 codon usage perspective (Fig. 6b, Supplementary file 3). To substantiate the factors  
268 governing this codon practice GC3 vs. Enc plot analysis was done. It has been proposed that,  
269 GC3-Enc plot of genes should be placed on or above the continuous Enc curve when only  
270 mutational pressure prevails. However, in the presence of translational selection, the plots  
271 should fall well below the aforementioned curve<sup>35</sup>. Here the GC3-Enc plots of protein-coding  
272 genes of all studied mitogenomes were below the curve designating the influence of  
273 translational selection over those genes. Hence, we conclude that, the codon usage pattern of  
274 *T. affinis* mitogenome along with other examined species is affected by the pervasiveness of  
275 translational selection over mutational pressure.

276 Moreover, values of WWC, SSU, WWU and SSC calculated from the RSCU tables for  
277 detecting the translational efficiency clearly indicated the preference of WWC and SSC over  
278 WWU and SSU. This pointed towards the selection of C between the pyrimidines (C or U) at  
279 the third position of codons. Calculated P2 values were greater than 0.5 for all the protein-  
280 coding genes in the investigated Leiothrichidae mitogenomes (Table 1, Supplementary file 3)  
281 signifying the pivotal role of translational efficiency in dictating the codon usage pattern.  
282 Translational selection along with translational efficiency plays a pivotal role in natural  
283 selection escorting towards codon preference<sup>35</sup>. Inclination towards translational efficiency  
284 also leads to favor codons matching with the restricted anticodon repertoire of mitochondrial  
285 tRNAs<sup>41</sup> enhancing their competence in the last phase of the central dogma. The nucleotide at  
286 the third degenerating position of the codon is responsible for the superlative codon-  
287 anticodon binding energy<sup>38</sup>. Previous studies have found that, U is preferred at the third  
288 position specifically when G or C is present in the first two positions. On the contrary, when  
289 the first two positions are taken by A or U; C is the 'right choice' (at third position)<sup>38</sup>. Thus,

290 translational efficiency can be characterized by the P2 index, which allows us to choose  
291 between the pyrimidines in codons with UU, UA, AA, AU, GG, GC, CG and CC in the first  
292 and second position. Results from this analysis clearly ( $p > 0.5$ ) validated the accountability  
293 of translational efficiency suggesting that those genes may have gone through several  
294 adaptations with rapid changes in their expression level. The cumulative effect of all these  
295 has enhanced the capability of mitochondrial metabolic processes substantiating boisterous  
296 nature of these birds. This result showed similarity with a previous study on Dragonflies  
297 where the increased mitochondrial capacity aided their elevated flight ability<sup>42</sup>.

### 298 **Comparative mitochondrial genomics**

299 The select mitogenomes were compared with *T. affinis* mitogenome (*do novo* assembled) for  
300 tRNA anticodons, start and stop codons, strand variability, intergenic and overlapping  
301 regions, GC/AT skew and RSCU (Supplementary file 3). The comparative anticodon analysis  
302 revealed an identical pattern of anticodon usages for all tRNAs among the investigated  
303 mitogenomes. Most of the protein-coding genes start with ATG in all the mitogenomes.  
304 AGG, AGA, TAG and TAA were identified as stop codons for most of the PCGs; however,  
305 in every mitogenome, there were some stop codons, which could not be perfectly identified  
306 (Supplementary file 3). Strand variation property showed an exact pattern among the studied  
307 mitogenomes Both rRNAs were on positive (+) strand. Except for nad6, all other PCGs were  
308 also on the positive (+) strand. While tRNA Q, tRNA N, tRNA C, tRNA Y, tRNA A, tRNA  
309 S2, tRNA P and tRNA E were located on the negative (-) strand, the other tRNAs were on  
310 positive (+) strand. RSCU based analysis revealed GCC(A), UGC(C), UUC(F), GGA(G),  
311 AAA(K), CUA(L), UUA(L), AUA(M), CCU(P), CAA (Q), AGC(S), UCC(S), ACC(T) and  
312 GUA(V) as optimal codons in the investigated mitogenomes. The comparative analysis of  
313 intergenic and overlapping regions also revealed identical pattern among studied  
314 mitogenomes. Intergenic regions were found between trnL2(taa) and nad1, nad1 and

315 trnI(gat), trnI(gat) and trnQ(ttg), nad2 and trnW(tca), trnA(tgc) and trnN(gtt), trnS2(tga) and  
316 trnD(gtc), trnD(gtc) and cox2, atp6 and cox3, nad3 and trnR(tcg), nad4 and trnH(gtg),  
317 trnL1(tag) and nad5, nad5 and cob, cob and trnT(tgt), trnT(tgt) and trnP(tgg) (CR1) along  
318 with trnP(tgg) and nad6 (Supplementary file 3). The intergenic region between trnT(tgt) and  
319 trnP(tgg) were longest ranging from 939 bp (*G. cineraceus*) to 1139bp (*G. albogularis*).  
320 Overlapping regions were much shorter, ranging from 2 to 5 bp (Supplementary file 3). The  
321 highest overlapping length was between nad4l and nad4 (4bp for *G. poecilorhynchus* voucher  
322 B33 and *T. affinis*, and 5 bp for other mitogenomes(Supplementary file 3). These characters  
323 revealed identical patterns for the aforementioned characteristics in the compared  
324 mitogenomes.

### 325 **Comparative tRNA structure analysis of *T. affinis de-novo* mitogenome**

326 The wobble base pairing which does not follow the Watson-Crick base pairing rule is of  
327 immense importance in studying the tRNA structure often substituting GC or AT base pairs  
328 contributing to thermodynamic stability<sup>43</sup>. All these features together affect several biological  
329 processes<sup>44</sup>. Studies have reported that, RNA binding proteins generally adhere to G-U sites  
330 differing from the Watson-Crick or other mis-matched base-pair pattern<sup>45</sup>. Hence, while  
331 understanding the exact functional features of mitogenomes, tRNA acts as a pivotal tool<sup>45,46</sup>.  
332 In *T. affinis*, all the tRNAs were folded into classic secondary clover-leaf structure. In *T.*  
333 *affinis*mitogenome, though Watson-Crick base pair dominated, wobble base pairs were also  
334 detected (Fig. 7). For instance, trnA, trnC, trn E, trnN, trnP, trnS1, trnS2 and trnY had wobble  
335 base pairing at the acceptor arm. Moreover, trnA, trnC, trnS1, trnQ, trnP and trnN contained  
336 wobble base pairing at TYC stem. Same G-U base pairs were also detected at the anticodon  
337 stem of trnC, trnP, trnQ, trnS1 and trnT. Three consecutive wobble base pairs were detected  
338 at DHU loop of trnS2. Along with, some other mismatched base pairs were also found in  
339 trnD, trnE, trnG, trnH, trnM and trnL2. Among other species considered in the present study,

340 all the tRNAs were found to be folded in clover-leaf structure with dominating Watson-Crick  
341 base pairing.

### 342 **Control region of *T. affinis* de-novo mitogenome**

343 Vertebrate mitochondrial Control Region (CR) is divided in to three domains (I, II and III)<sup>46</sup>.  
344 Domain I contains three Extended Terminal Associated Sites (ETAS) proceeded by a C-rich  
345 region. Domain II contains F-box, E-box, D-box, C-box and B-box<sup>47</sup>. For birds, there is a  
346 special Bird Similarity Box (BSB) present in the left side of B-box in domain II. Domain III  
347 consists of three conserved sequence blocks (CSB-I, II, III). Domain III also contains  
348 replication origin of H-strand along with bi-directional promoters for both H- and L-strand  
349 transcription. Domain II is supposed to be more conserved than Domain I and III<sup>47</sup>. Among  
350 all the investigated species of Leiothrichidae family, a duplication of CR was observed. All  
351 the aforementioned domains and conserved boxes were identified through sequence  
352 alignment. Conserved BSB was prominent in both CR1 and CR2 (Fig. 8). No tandem repeats  
353 were found among the CRs. Duplication of CR region is important in regulation of  
354 replication and transcription within mitochondrial genome<sup>46</sup>. Moreover, duplicated CR is also  
355 associated with extended longevity of bird species<sup>48</sup>. Thus, the present study reported the  
356 genetic features of duplicated CR among select Leiothrichidae members including *T. affinis*,  
357 which will further be helpful in evolutionary analysis of this group.

### 358 **Evolutionary analysis**

359 Genetic and evolutionary distance calculation revealed higher K2P distance in nad2, atp8 and  
360 nad6 whereas cox1 possessed the lowest value among the Leiothrichidae family (Fig. 9).  
361 Regarding the ka/ks analysis, the average synonymous substitution rate (Ks) for nd2 gene  
362 was highest whereas non-synonymous substitution rate (ka) was highest for atp8.  $\square$ (ka/ks)  
363 values of the protein-coding genes ranged from 0.014 to 0.183 and was in the following  
364 order- cox1<cox3<nad1<cob<nad4l<atp6<nad4<cox2<nad3<nad5<nad6<nad2<atp8

365 (Supplementary file 3). Lowest K2P distance for *cox1* gene indicated towards its conserved  
366 nature among the Leiothrichidae family. Moreover, this also implicated the preference of  
367 NADH:ubiquinoneoxidoreductase (complex I) over the succinate dehydrogenase complex in  
368 electron transport chain all through the examined family. Complex I is responsible for  
369 exporting four H<sup>+</sup> ion out of the mitochondrial matrix participating in the generation of H<sup>+</sup>  
370 gradient across the mitochondrial membrane, which ultimately speeds up ATP generation  
371 whereas this mechanism is totally absent when complex II is used<sup>49</sup>. Moreover, the non-  
372 synonymous substitution rate of *cox1* was also found to be least, indicating its conserved  
373 nature in mitochondrial machinery of Leiothrichidae family. Mitochondria associated NADH  
374 dehydrogenase 2 encoded by the *nad2* gene is also a subunit of complex 1 located in the inner  
375 mitochondrial membrane and is the largest complex of ETS<sup>49</sup>. The high synonymous  
376 substitution rate (Ks) of *nad2* gene further indicated the preserved amino acid component of  
377 complex I. Highest Ka value of *atp8* pointed to a highly variable nature of this protein  
378 indicating the erratic nature of mitochondrial *atp8* among vertebrates<sup>50</sup>. The  $\frac{ka}{ks}$  values  
379 of all the protein-coding genes were <1 suggesting the persistence of purifying selection  
380 against deleterious mutation. Thus, the evolutionary analysis aided in understanding the  
381 influence of natural selection manipulating species evolution along with the interaction  
382 between selection and mutational pressure responsible for protein evolution which has been  
383 already suggested<sup>39</sup>.

## 384 **Conclusion**

385 We report for the first time the complete mitogenome of *Turdoides affinis*(MN848144). We  
386 find the *de-novo* assembly approach more appropriate than a reference-based assembly  
387 approach. The comparative mitogenomics of the Leiothrichidae family reveals their  
388 preference towards AT-rich codons as well as the persistence of translational efficiency.  
389 tRNA analysis shows the dominance of Watson-Crick base pairing with a few exceptions of



390 wobble base pairing. Duplicated control regions are found among Leiothrichidae family  
391 mitogenomes that may help in their extended longevity. Evolutionary analysis confirms  
392 that protein-coding genes are under purifying selection pressure. Genetic distance and  
393 variation analysis indicate the dominance of NADH dehydrogenase complex-I in the electron  
394 transport system of *T. affinis*. Our limited phylogenetics results suggest that *T. Affinis* is closer  
395 to *Garrulax*.

396 **References**

- 397 1. Bock, W. J. A generic review of the family Ardeidae (Aves). American Museum novitates;  
398 no. 1779 American Museum of Natural History (1956).
- 399 2. Howard, R. & Alick M. A complete checklist of the birds of the world. Edition-2.  
400 Academic Press Ltd (1991).
- 401 3. Monroe, B. L. & Charles G. S. A world checklist of birds. Yale University Press (1997).
- 402 4. Zou, Y., Jing, M. D., Bi, X. X., Zhang, T. & Huang, L. The complete mitochondrial  
403 genome sequence of the little egret (*Egretta garzetta*). *Genet. Mol. Biol.* **38**, 162-172 (2015).
- 404 5. Ingman, M., Kaessmann, H., Pääbo, S. & Gyllensten, U. Mitochondrial genome variation  
405 and the origin of modern humans. *Nature*. **408**, 708 (2000).
- 406 6. Sheldon, F. H. Rates of single-copy DNA evolution in herons. *Mol. Biol. Evol.* **4**, 56-69  
407 (1987).
- 408 7. Gentile, G., Fabiani, A., Marquez, C., Snell, H. L., Snell, H. M., Tapia, W. & Sbordoni, V.  
409 An overlooked pink species of land iguana in the Galápagos. *PNAS*. **106**, 507-511 (2009).
- 410 8. Zhang, P. & Wake, D. B. Higher-level salamander relationships and divergence dates  
411 inferred from complete mitochondrial genomes. *Mol. Phylogenetics Evol.* **53**, 492-508 (2009).
- 412 9. Pacheco, M. A., Battistuzzi, F. U., Lentino, M., Aguilar, R. F., Kumar, S. & Escalante, A.  
413 A. Evolution of modern birds revealed by mitogenomics: timing the radiation and origin of  
414 major orders. *Mol. Biol. Evol.* **28**, 1927-1942 (2011).
- 415 10. Hitoshi, S., Nunome, M., Kinoshita, G., Aplin, K. P., Vogel, P., Kryukov, A. P. & Jin,  
416 M. Evolutionary and dispersal history of Eurasian house mice *Mus musculus* clarified by  
417 more extensive geographic sampling of mitochondrial DNA. *Heredity*. **111**, 375-377 (2013).

- 418 11. Campbell, V. & Lapointe, F. J. Retrieving a mitogenomic mammal tree using composite  
419 taxa. *Mol. Phylogenetics Evol.* **58**, 149-156 (2011).
- 420 12. Jamie, G.A. & de Silva G.E.H.A.N. Similarity of the calls of juvenile pied cuckoo  
421 *Clamator jacobinus* and its Sri Lankan host species, yellow-billed babbler *Turdoides affinis*.  
422 *Forktail*, **30**,133-134 (2014).
- 423 13. Howard, R. & Moore, A. A complete checklist of the birds of the world (No. Ed. 2).  
424 Academic Press Ltd. (1991).
- 425 14. Cibois, A., Gelang, M., Alström, P., Pasquet, E., Fjeldså, J., Ericson, P. G. & Olsson, U.  
426 Comprehensive phylogeny of the laughingthrushes and allies (Aves, Leiothrichidae) and a  
427 proposal for a revised taxonomy. *Zool. Scr.* **47**, 428-440 (2018).
- 428 15. Miller, M. J. HBW and BirdLife International Illustrated Checklist of the Birds of the  
429 World Volume 2: Passerines Josep del Hoyo, Nigel J. Collar. 2016. Lynx Edicions,  
430 Barcelona. *J. Field Ornithol.* **88**, 421-424 (2017).16. Cibois, A., Gelang, M. & Pasquet, E.  
431 An overview of the babblers and associated groups. *Syst. Notes on Asian Birds.* **68**, 1-5  
432 (2010).
- 433 17. Rasmussen, P. C. & Anderton C. J. Birds of south Asia: the Ripley guide. Washington,  
434 DC, *British Birds.* **98**, 609-613 (2005).
- 435 18. Zacharias, V. J & Mathew, D.N. Behaviour of the Whiteheaded Babbler *Turdoides affinis*  
436 Jerdon. *J. Bombay Nat. Hist. Soc.* **95**, 8-14 (1998).
- 437 19. Gaston, A. J., Matthew, D. N. & Zacharias, V. J. Regional variation in the breeding  
438 seasons of Babblers in India. *Ibis.* **121**, 512-516 (1979).

- 439 20. Huang, R., Zhou, Y., Yao, Y., Zhao, B., Zhang, Y. & Xu, H. L. Complete mitochondrial  
440 genome and phylogenetic relationship analysis of *Garrulax affinis* (Passeriformes,  
441 Timaliidae). *Mitochondrial DNA Part A*. **27**, 3502-3503 (2016).
- 442 21. Xue, H., Zhang, H., Li, Y., Wu, X., Yan, P. & Wu, X. B. The complete mitochondrial  
443 genome of *Garrulax cineraceus* (Aves, Passeriformes, Timaliidae). *Mitochondrial DNA Part*  
444 *A*. **27**, 147-148 (2016).
- 445 22. Zhou, Y., Wei, D., Qi, Y., Xu, H., Li, D., Ni, Q. & Yao, Y. Complete mitochondrial  
446 genome of *Garrulax elliotii* (Passeriformes, Timaliidae). *Mitochondrial DNA Part A*. **27**,  
447 3687-3688 (2016).
- 448 23. Huan, Z., Yao, Y., Zhou, Y., Qi, Y., Wang, Q., Li, D. & Xu, H. Complete mitochondrial  
449 genome sequence of *Garrulax formosus* (Aves, Passeriformes, Timaliidae) and its  
450 phylogenetic analysis. *Mitochondrial DNA Part A*. **27**, 2858-2859 (2016).
- 451 24. Zhou, Y., Qi, Y., Xu, H., Huan, Z., Li, D., Xie, M. & Yao, Y. The complete  
452 mitochondrial genome sequence of *Garrulax ocellatus* (Aves, Passeriformes, Timaliidae).  
453 *Mitochondrial DNA Part A*. **27**, 2689-2690 (2016).
- 454 25. Zhang, H., Li, Y., Wu, X., Xue, H., Yan, P. & Wu, X. B. The complete mitochondrial  
455 genome of *Garrulax perspicillatus* (Passeriformes, Timaliidae). *Mitochondrial DNA Part A*.  
456 **27**, 1265-1266 (2016).
- 457 27. Zhou, Y. Y., Qi, Y., Yao, Y. F., Huan, Z. J., Li, D. Y., Xie, M. & Xu, H. L.  
458 Characteristic of complete mitochondrial genome and phylogenetic relationship of *Garrulax*  
459 *sannio* (Passeriformes, Timaliidae). *Mitochondrial DNA Part A*. **27**, 2947-2948 (2016).
- 460 26. Qi, Y., Zhou, Y. Y., Yao, Y. F., Huan, Z. J., Li, D. Y., Xie, M. & Xu, H. L. The  
461 complete mitochondrial genome sequence of *Garrulax poecilorhynchus* (Aves,  
462 Passeriformes, Timaliidae). *Mitochondrial DNA Part A*. **27**, 3636-3637 (2016).

- 463 28. Zhao, Q., Xu, H. L. & Yao, Y. F. The complete mitochondrial genome and phylogeny of  
464 the Emei Shan liocichla (*Liocich laomeiensis*). *Conserv. Genet. Resour.* **11**, 303-307(2018).
- 465 29. Li, B., Yao, Y., Li, D., Ni, Q., Zhang, M., Xie, M. & Xu, H. Complete mitochondrial  
466 genome of *Minla ignotincta* (Passeriformes: Timaliidae). *Mitochondrial DNA Part B.* **1**, 140-  
467 141 (2016).
- 468 30. Vaser, R., Sović, I., Nagarajan, N. & Šikić, M. Fast and accurate de novo genome  
469 assembly from long uncorrected reads. *Gen. Res.* **27**, 737-746 (2017).
- 470 31. Baker, M. *De novo* genome assembly: what every biologist should know. *Nat. Methods.*  
471 **9**, 333–337(2012).
- 472 32. Martin, M. Cutadapt removes adapter sequences from high-throughput sequencing reads.  
473 *EMBnet. journal.* **17**, 10-12 (2011).
- 474 33. Stothard, P. & Wishart, D. S. Circular genome visualization and exploration using  
475 CGView. *Bioinformatics.* **21**, 537-539 (2004).
- 476 34. Zhou, X., LinQ, F. W & Chen, X. The complete mitochondrial genomes of sixteen  
477 ardeid birds revealing the evolutionary process of the gene rearrangements. *BMC Genomics.*  
478 **15**, 573 (2014).
- 479 35. Peden, J. CodonW. Thesis submitted to Trinity College. (1997).
- 480 36. Perna, N. T. & Kocher, T. D. Patterns of nucleotide composition at fourfold degenerate  
481 sites of animal mitochondrial genomes. *J. Mol. Evol.* **41**, 353-358 (1995).
- 482 37. Li, Q., Wang, Q., Jin, X., Chen, Z., Xiong, C., Li, P., Liu, Q. & Huang, W.  
483 Characterization and comparative analysis of six complete mitochondrial genomes from  
484 ectomycorrhizal fungi of the *Lactarius* genus and phylogenetic analysis of the  
485 Agaricomycetes. *Int.J.Biol.Macromol.* **121**, 249-260 (2019).

- 486 38. Wang, L., Xing, H., Yuan, Y., Wang, X., Saeed, M., Tao, J. & Sun, X. Genome-wide  
487 analysis of codon usage bias in four sequenced cotton species. *PLoS one*. **13**, e0194372  
488 (2018).
- 489 39. Roy, A., Mukhopadhyay, S., Sarkar, I. & Sen, A. Comparative investigation of the  
490 various determinants that influence the codon and amino acid usage patterns in the genus  
491 *Bifidobacterium*. *World J. Microbiol. Biotechnol.* **31**, 959-981 (2015).
- 492 40. Rozas, J., Sánchez-DelBarrio, J. C., Messeguer, X. & Rozas, R. DnaSP, DNA  
493 polymorphism analyses by the coalescent and other methods. *Bioinformatics*. **19**, 2496-2497  
494 (2003).
- 495 41. Jia, W. & Higgs, P. G. Codon usage in mitochondrial genomes: distinguishing context-  
496 dependent mutation from translational selection. *Mol. Biol. Evol.* **25**, 339-351 (2007).
- 497 42. Guan, D. L., Qian, Z. Q., Ma, L. B., Bai, Y. & Xu, S. Q. Different mitogenomic codon  
498 usage patterns between damselflies and dragonflies and nine complete mitogenomes for  
499 odonates. *Sci.Rep.* **9**, 678-683 (2019).
- 500 43. Crick, F. H. C. Codon-anticodon pairing: The wobble hypothesis. *J. Mol. Biol.* **19**, 548-  
501 555 (1966).
- 502 44. Varani, G. & McClain, W. H. The G-U wobble base pair: A fundamental building block  
503 of RNA structure crucial to RNA function in diverse biological systems. *EMBO Rep.* **1**, 18-  
504 23 (2000).
- 505 45. Takashi, P. S., Miya, M., Mabuchi, K. & Nishida, M. Structure and variation of the  
506 mitochondrial genome of fishes. *BMC Genomics*. **17**, 719 (2016).
- 507 46. Kundu, S., Kumar, V., Tyagi, K., Chakraborty, R., Singha, D., Rahaman, I., Pakrashi, A.  
508 & Chandra, K. Complete mitochondrial genome of Black Soft-shell Turtle (*Nilssonina*

509 *nigricans*) and comparative analysis with other Trionychidae. *Sci.Rep.* **8**, 17378-17389  
510 (2018).

511 47. Ruokonen, M. & Kvist, L. Structure and evolution of the avian mitochondrial control  
512 region. *Mol.Phyl.Evol.* **23**, 422–432 (2002).

513 48. Skujina, I., McMahon, R., Lenis, V.P.E., Gkoutos, G.V. & Hegarty, M. Duplication of  
514 the mitochondrial control region is associated with increased longevity in birds. *Aging.* **8**,  
515 1781-1785 (2016).

516 49. Berg M.J., Tymoczko L. J. & Stryer, L. Oxidative Phosphorylation in Eukaryotes Takes  
517 Place in Mitochondria. *Biochemistry.* **5th edition**, New York: W H Freeman, (2002).

518 50. Kumar, S. Patterns of nucleotide substitution in mitochondrial protein-coding genes of  
519 vertebrates. *Genetics.* **143**, 537-548 (1996).

## 520 **Acknowledgments**

521 We thank the Ministry of Environment, Forest and Climate Change, Govt. of India for  
522 financial support. We are also thankful to the Tamil Nadu Forest Department for providing  
523 the permissions and support to conduct the study.

## 524 **Author Contribution**

525 RPS collected samples and conceived the idea. RPS, SKS, PD and SDR designed the  
526 experiments and generated DNA data. IS analysed the data. RPS and IS wrote the manuscript  
527 and generated all the figures. All authors reviewed the manuscript.

## 528 **Additional Information**

## 529 **Competing interests**

530 The author(s) declare no competing interests

## 531 **Figure legends**

532 **Figure legends**

533 **Figure 1.** Map showing sample collection area.

534 **Figure 2.** The mitochondrial genome view of *Turdoides affinis*. Gene transcription direction  
535 is indicated by arrows. Colour codes are indicated at the right upper side of the figure. tRNAs  
536 are indicated with the single letter code of amino acids. Black sliding window indicated the  
537 GC content of all the regions. GC skew has been plotted through green and violet colour  
538 sliding windows. The figure was drawn by CGView Online server  
539 ([http://stothard.afns.ualberta.ca/cgview\\_server/](http://stothard.afns.ualberta.ca/cgview_server/)) using default parameters. The photograph of  
540 *Turdoides affinis* was taken by the first author and was edited with Paint.net.

541 **Figure 3.** Phylogenetic tree based on complete mitogenome (*De-novo* assembled *Turdoides*  
542 *affinis* mitogenome). Maximum likelihood method with 1000 bootstrap value along with  
543 Kimura 2- parameter was used to generate the phylogenetic tree.

544 **Figure 4.** Comparison of gene orders among select complete mitogenomes of Leiothrichidae  
545 family. Organisms names are abbreviated as: ta - *Turdoides affinis*, ga - *Garrulax affinis*  
546 (KT182082.1), gal - *Garrulax albogularis* (KX082660.1), gcVA - *Garrulax canorus* voucher  
547 AHNU:A0040 (JQ348398.1), gc - *Garrulax canorus* (KT633399.1) , gci - *Garrulax*  
548 *cineraceus* (KF926988.1), ge - *Garrulax elliotii* (KT272404.1), gf - *Garrulax formosus*  
549 voucher B36 (KR020504.1), go - *Garrulax ocellatus* (KP995195.1), gp - *Garrulax*  
550 *perspicillatus* (KF997865.1), gpVB - *Garrulax poecilorhynchus* voucher B33 (KR909134.1),  
551 gsVG - *Garrulax sannio* voucher GSAN20150704V3 (KT373847.1), gs - *Garrulax sannio*  
552 (KR869824.1), la - *Leiothrix argentauris* (HQ690245.1), ll - *Leiothrix lutea* (JQ423933.1), lo  
553 - *Liocichla omeiensis* (KU886092.1), mi - *Minla ignotincta* (KT995474.1), tm -  
554 *Trochalopteron milnei* (MH238447.1). Genes were found arranged in an identical fashion  
555 except for gs and gsVG.

556 **Figure 5.** Nucleotide composition of *Turdoides affinis* mitogenome. (a) Position-specific  
557 nucleotide usage in *Turdoides affinis* mitogenome. This result was validated by the (b)



558 roseplot based on codon usage of *Turdoides affinis* mitogenome. (c) roseplot based on amino  
559 acid usage of *Turdoides affinis* mitogenome. Heatmaps based on (d) codon usage and (e)  
560 amino acid usage.

561 **Figure 6.** (a) ENc vs GC3 plot revealed the presence of translational selection pressure on the  
562 PCGs of select Leiothrichidae family mitogenomes, (b) RSCU analysis of *Turdoides affinis*  
563 mitogenome. X-axis represents the codon families with different colour patches. Cumulative  
564 codon fraction is plotted on Y-axis.

565 **Figure 7.** Putative secondary structures of *Turdoides affinis* tRNAs. tRNAs are specified  
566 with respective single letter amino acid codes.

567 **Figure 8.** Domains and boxes identified in (a) CR1 and (b) CR2 of select Leiothrichidae  
568 family mitogenomes. Regions of the identified boxes are given at the lower part of each box.

569 **Figure 9.** Genetic and evolutionary distance among the PCGs of select species of the  
570 Leiothrichidae family. (a) K2P distance calculation, (b) Ks values, (c) Ka values and (d) Ka/Ks  
571 values of mitochondrial PCGs among investigated species of Leiothrichidae family.

572 **Supplementary file 1.** Description of complete mitogenome of *Turdoides affinis* assembled  
573 through reference based method.

574 **Supplementary file 2.** Phylogenetic tree with complete mitogenome of *Turdoides affinis*  
575 (reference based assembly).

576 **Supplementary file 3.** Comparative mitogenomics among compared Leiothrichidae family  
577 mitogenomes.

578

579

580

581

582

583 **Table 1.** Properties of complete mitogenome of *Turdoides affinis* assembled using *de-novo*  
584 assembly approach

Locus Name	Start	Stop	Strand	Length	Intergenic nucleotides	Anti Codon	WC_codon	Initiation codon	Termination Codon	P2 value
trnF(ttc)	1	68	+	68	-1	GAA	UUC	-	-	-
rrnS	68	865	+	798	-1	-	-	-	-	-
trnV(gta)	865	933	+	69	0	UAC	GUA	-	-	-
rrnL	934	2524	+	1591	0	-	-	-	-	-
trnL2(tta)	2525	2599	+	75	34	UAA	UUA	-	-	-
nad1	2634	3581	+	948	18	-	-	ATG	TAA	0.99
trnI(atc)	3600	3670	+	71	7	UCG	AUC	-	-	-
trnQ(caa)	3678	3747	-	70	-1	UUG	CAA	-	-	-
trnM(atg)	3747	3815	+	69	0	CAU	AUG	-	-	-
nad2	3816	4841	+	1026	14	-	-	ATG	TAA	0.97
trnW(tga)	4856	4925	+	70	1	UCA	UGA	-	-	-
trnA(gca)	4927	4995	-	69	10	UGC	GCA	-	-	-
trnN(aac)	5006	5078	-	73	1	GUU	AAC	-	-	-
trnC(tgc)	5080	5145	-	66	0	GCA	UGC	-	-	-
trnY(tac)	5146	5215	-	70	10	GUA	UAC	-	-	-
cox1	5226	6758	+	1533	0	-	-	ATG	TAG	0.97
trnS2(tca)	6759	6831	-	73	4	UGA	UCA	-	-	-
trnD(gac)	6836	6904	+	69	10	GUC	GAC	-	-	-
cox2	6915	7583	+	669	16	-	-	ATG	TAA	0.98
trnK(aaa)	7600	7669	+	70	1	UUU	AAA	-	-	-
atp8	7671	7832	+	162	-4	-	-	ATG	TAA	0.99
atp6	7829	8509	+	681	11	-	-	ATG	TAA	0.96

cox3	8521	9303	+	783	1	-	-	ATG	TAA	0.98
trnG(gga)	9305	9373	+	69	0	UCC	GGA	-	-	-
nad3	9374	9733	+	360	2	-	-	ATG	TAA	0.95
trnR(cga)	9724	9793	+	70	-10	UCG	CGA	-	-	-
nad4l	9795	10088	+	294	-4	-	-	ATG	TAA	0.99
nad4	10085	11449	+	1365	10	-	-	ATG	TAG	0.97
trnH(cac)	11460	11529	+	70	0	GUG	CAC	-	-	-
trnS1(agg)	11530	11595	+	66	-1	GCU	AGC	-	-	-
trnL1(cta)	11595	11665	+	71	21	UAG	CUA	-	-	-
nad5	11687	13471	+	1785	21	-	-	ATG	TAA	0.94
cob	13493	14626	+	1134	12	-	-	ATG	TAA	0.96
trnT(aca)	14639	14707	+	69	1138 (CR1)	UGU	ACA	-	-	-
trnP(cca)	15846	15914	-	69	9	UGG	CCA	-	-	-
nad6	15924	16439	-	516	0	-	-	ATG	TAA	0.97
trnE(gaa)	16440	16512	-	73	-	UUC	GGA	-	-	-
control region (CR2)	16513	17671	-	1159	-	-	-	-	-	-

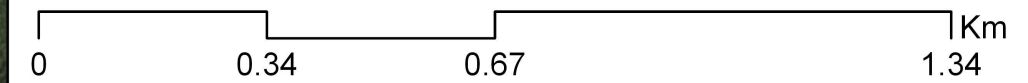
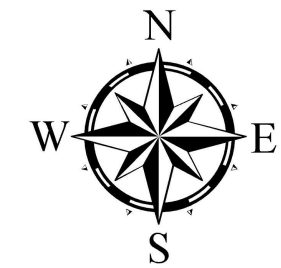
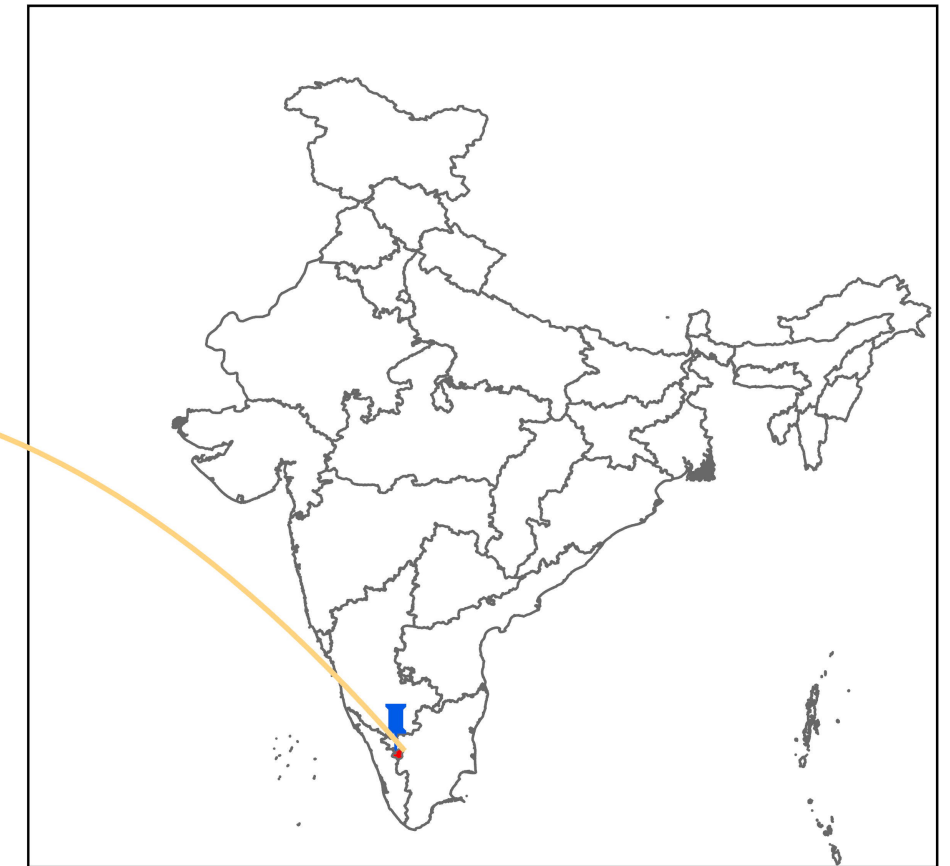
585

586

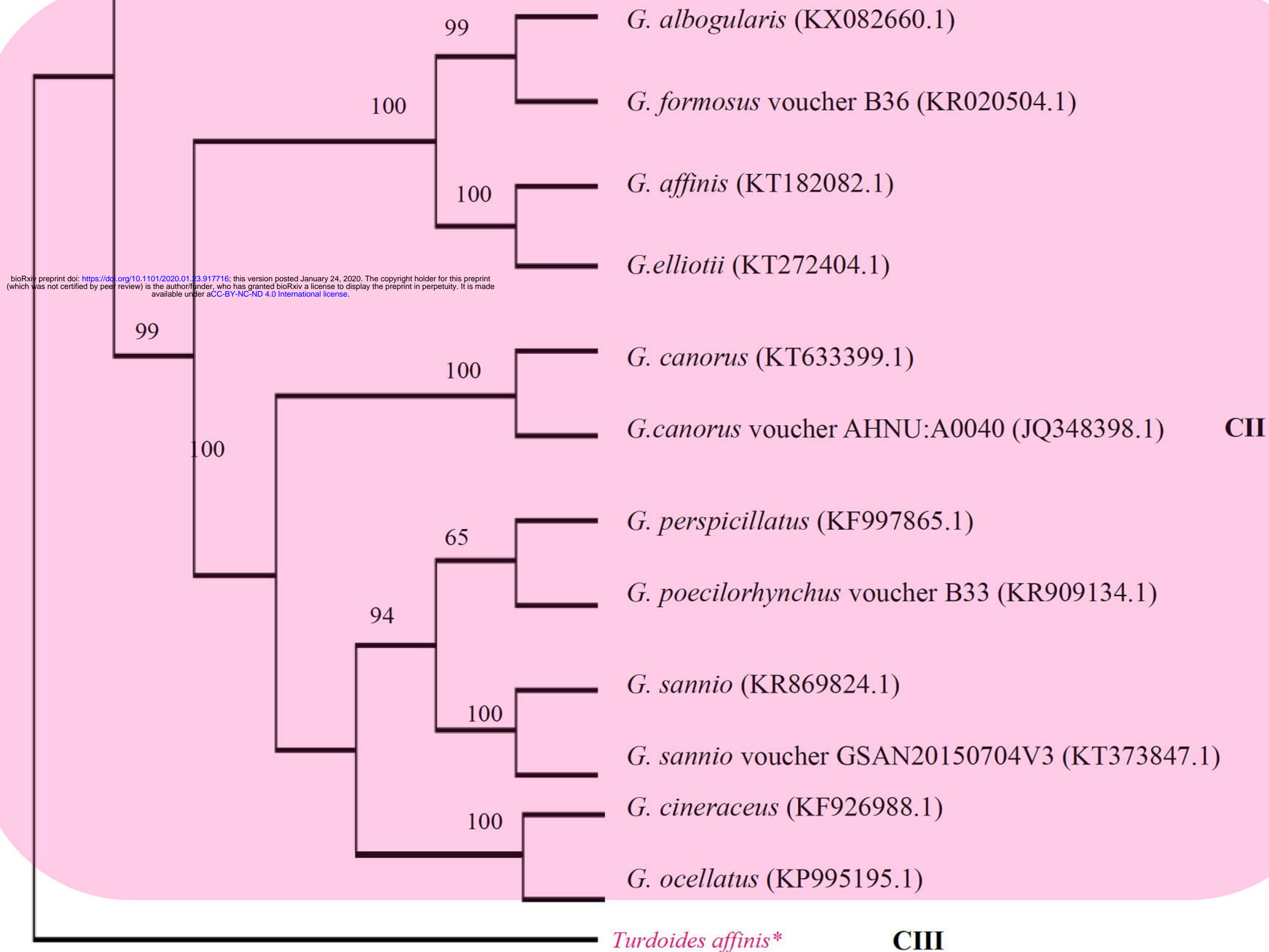
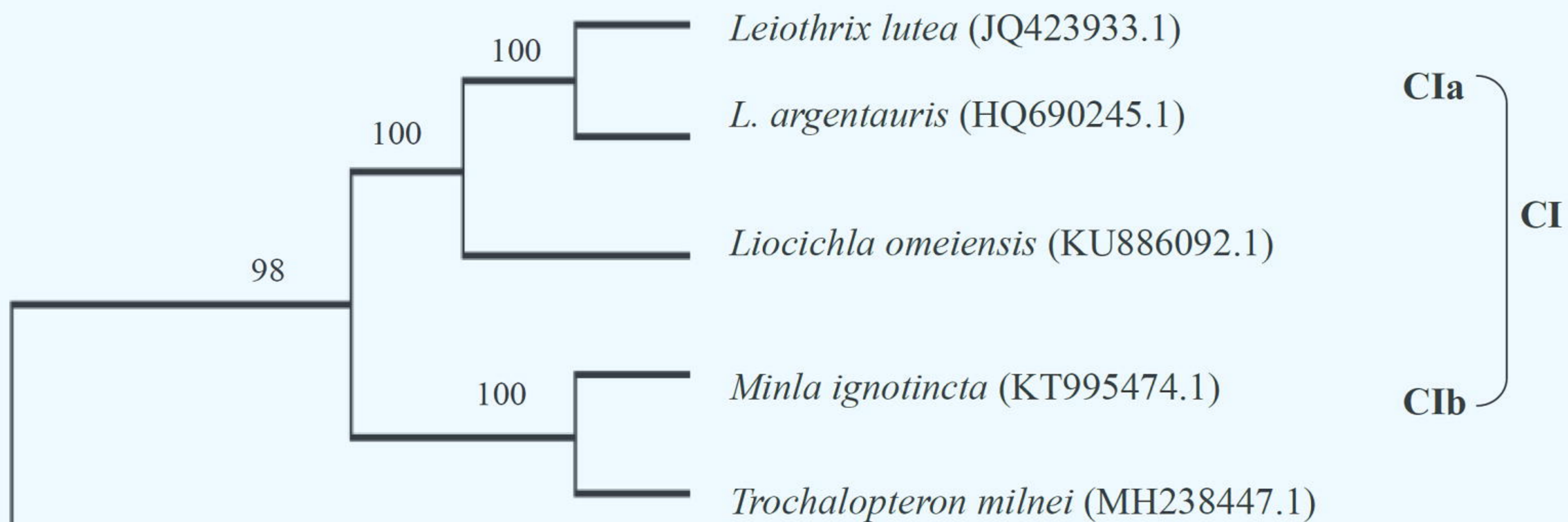
587 Table 2. List of complete mitochondrial genomes used for comparative mitogenomics study.  
588

Species	Accession No.	Total length	AT skew	GC skew	PCG no.	tRNA no.
<i>Turdoides affinis</i>	MN848144	17,671	0.13	-0.38	13	22
<i>Garrulax affinis</i>	KT182082.1	17856	0.10	-0.39	13	22
<i>Garrulax albogularis</i>	KX082660.1	17870	0.12	-0.40	13	22
<i>Garrulax canorus</i>	KT633399.1	17828	0.11	-0.38	13	22
<i>Garrulax canorus</i> voucher AHNU:A0040	JQ348398.1	17785	0.11	-0.38	13	22
<i>Garrulax elliotii</i>	KT272404.1	17873	0.10	-0.38	13	22
<i>Garrulax cineraceus</i>	KF926988.1	17800	0.11	-0.38	13	22
<i>Garrulax formosus</i> voucher B36	KR020504.1	17869	0.10	-0.38	13	22
<i>Garrulax ocellatus</i>	KP995195.1	17828	0.11	-0.37	13	22
<i>Garrulax perspicillatus</i>	KF997865.1	17873	0.10	-0.38	13	22
<i>Garrulax poecilorhynchus</i> voucher B33	KR909134.1	17814	0.11	-0.39	13	22
<i>Garrulax sannio</i>	KR869824.1	17840	0.11	-0.37	13	22
<i>Garrulax sannio</i> voucher GSAN20150704V3	KT373847.1	17848	0.11	-0.37	14	22
<i>Leiothrix argentauris</i>	HQ690245.1	17833	0.11	-0.37	13	22
<i>Leiothrix lutea</i>	JQ423933.1	17615	0.11	-0.38	13	22
<i>Liocichla omeiensis</i>	KU886092.1	17830	0.11	-0.37	13	22
<i>Minla ignotincta</i>	KT995474.1	17868	0.11	-0.38	13	22
<i>Trochalopteron milnei</i>	MH238447.1	17871	0.10	-0.38	13	22

589







bioRxiv preprint doi: <https://doi.org/10.1101/2020.01.23.917716>; this version posted January 24, 2020. The copyright holder for this preprint (which was not certified by peer review) is the author/funder, who has granted bioRxiv a license to display the preprint in perpetuity. It is made available under aCC-BY-NC-ND 4.0 International license.





### Position specific nucleotide usage

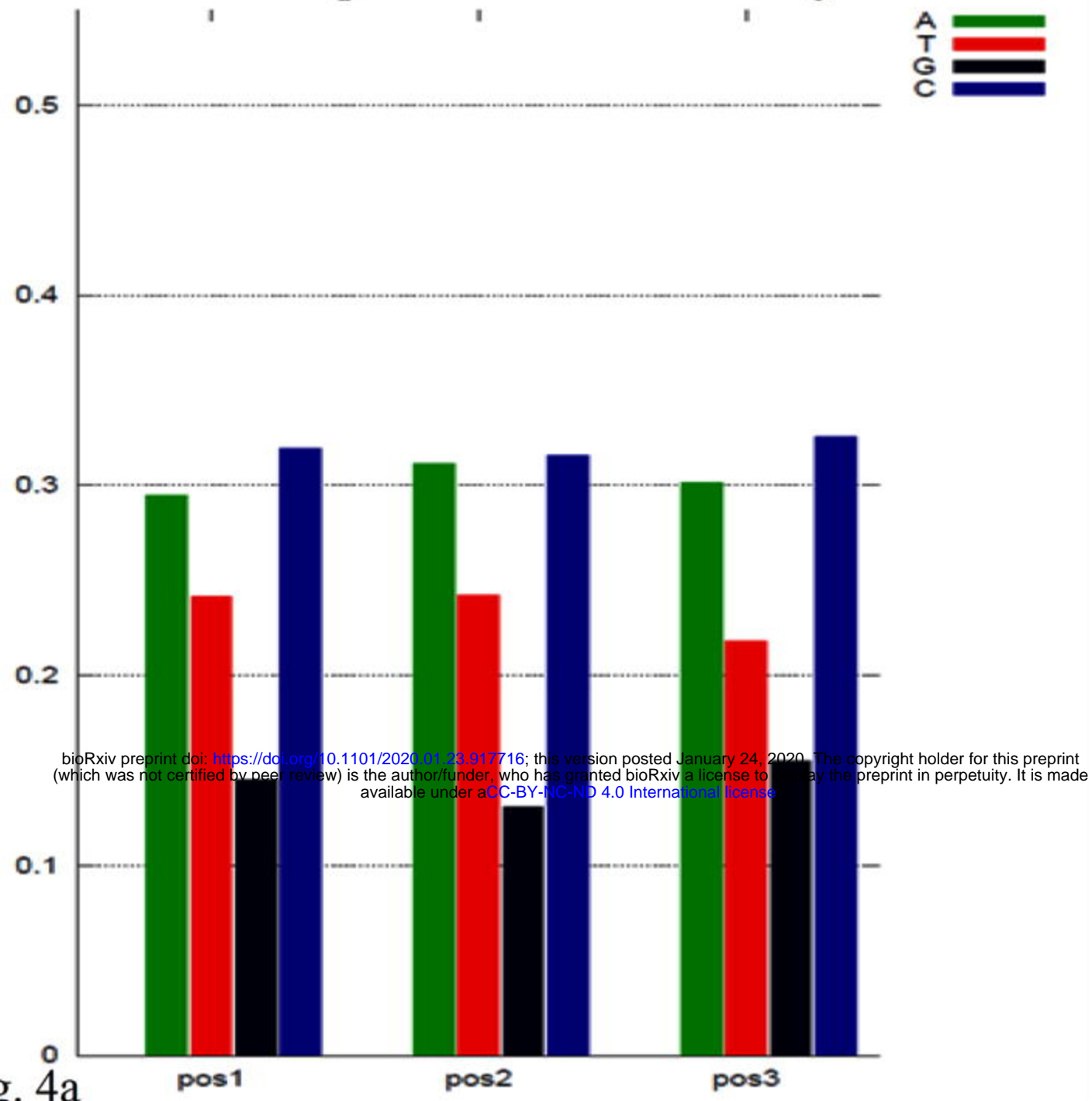


Fig. 4a

### Codon Usage

*Turdodes affinis*

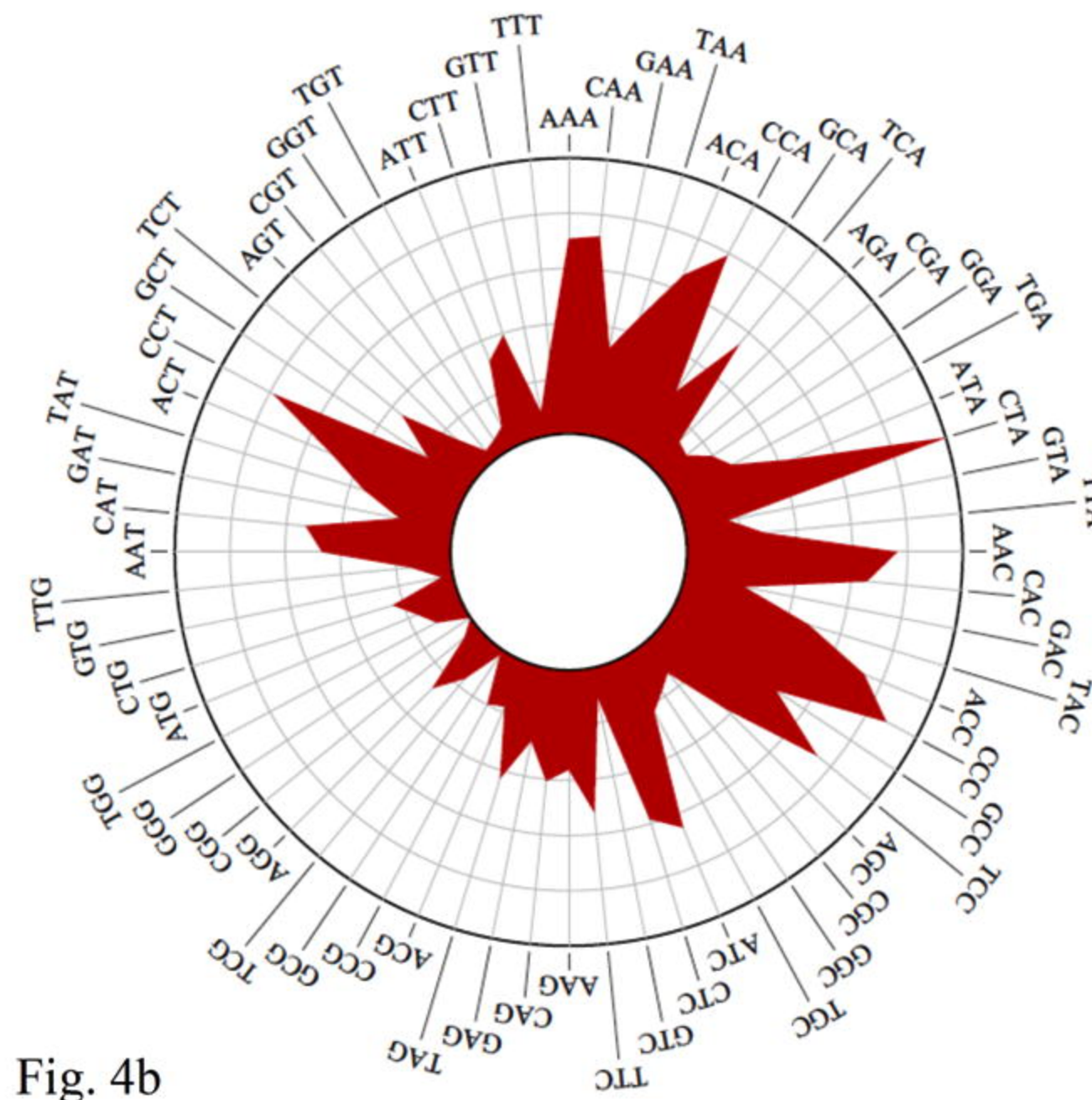


Fig. 4b

### Amino acid Usage

*Turdodes affinis*

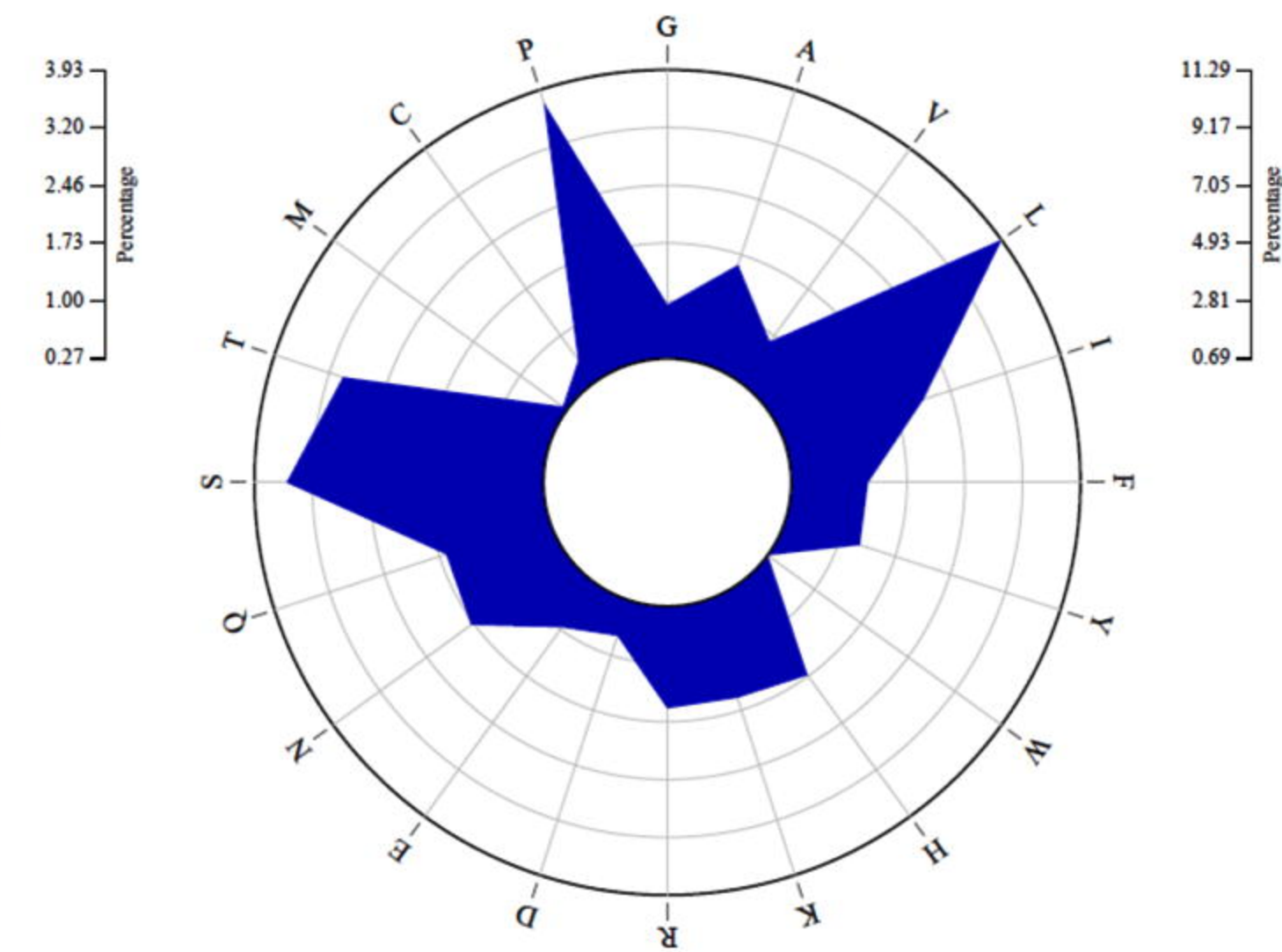
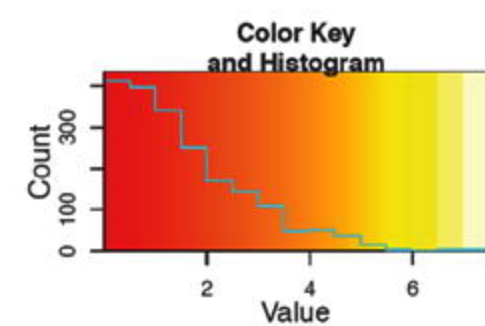


Fig. 4c

### Heat-map based on codon usage



### Heat-map based on amino acid usage

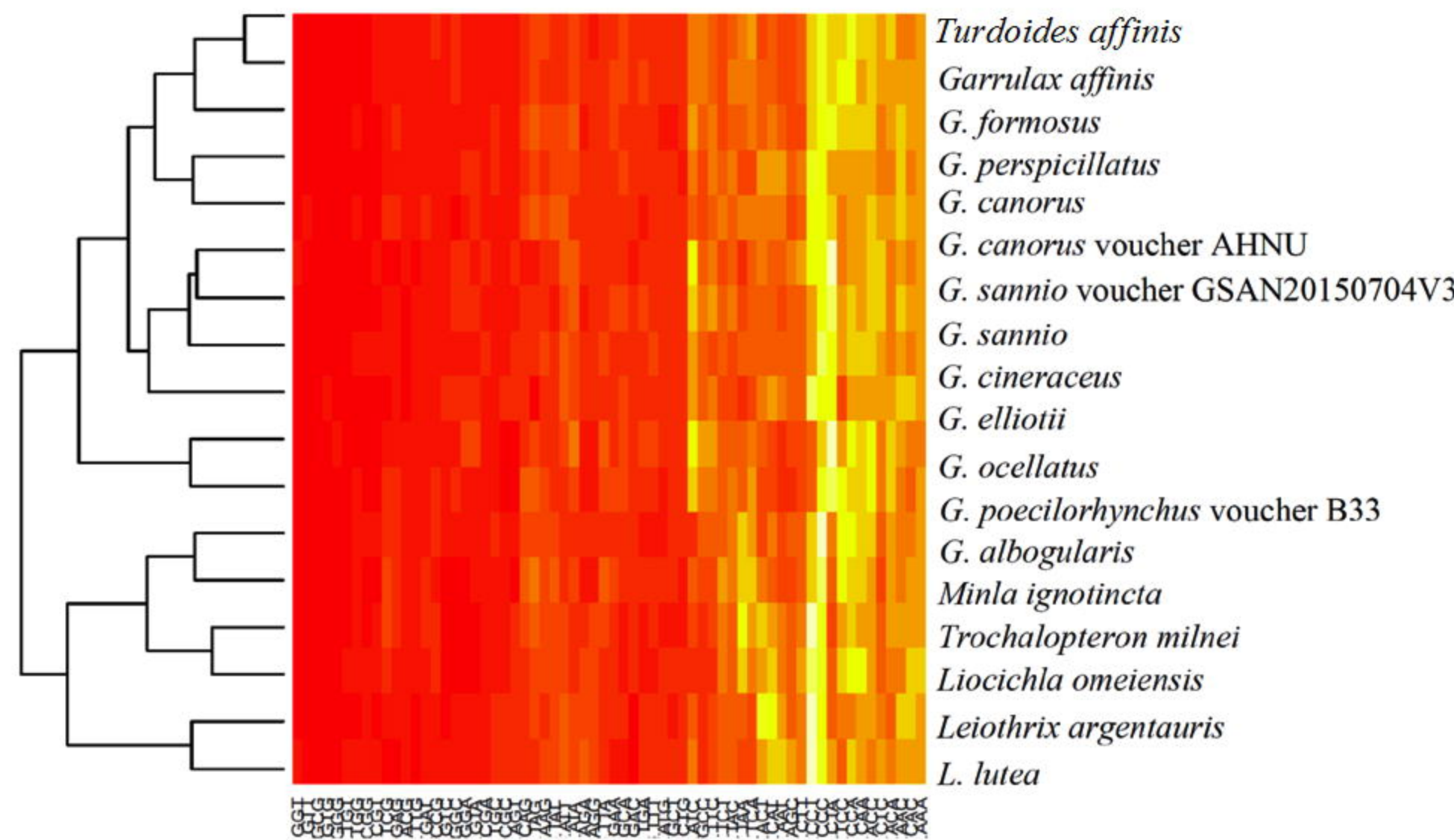
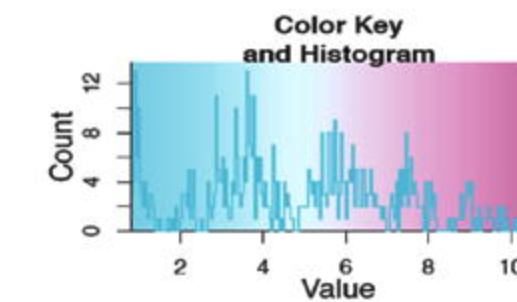


Fig. 4d

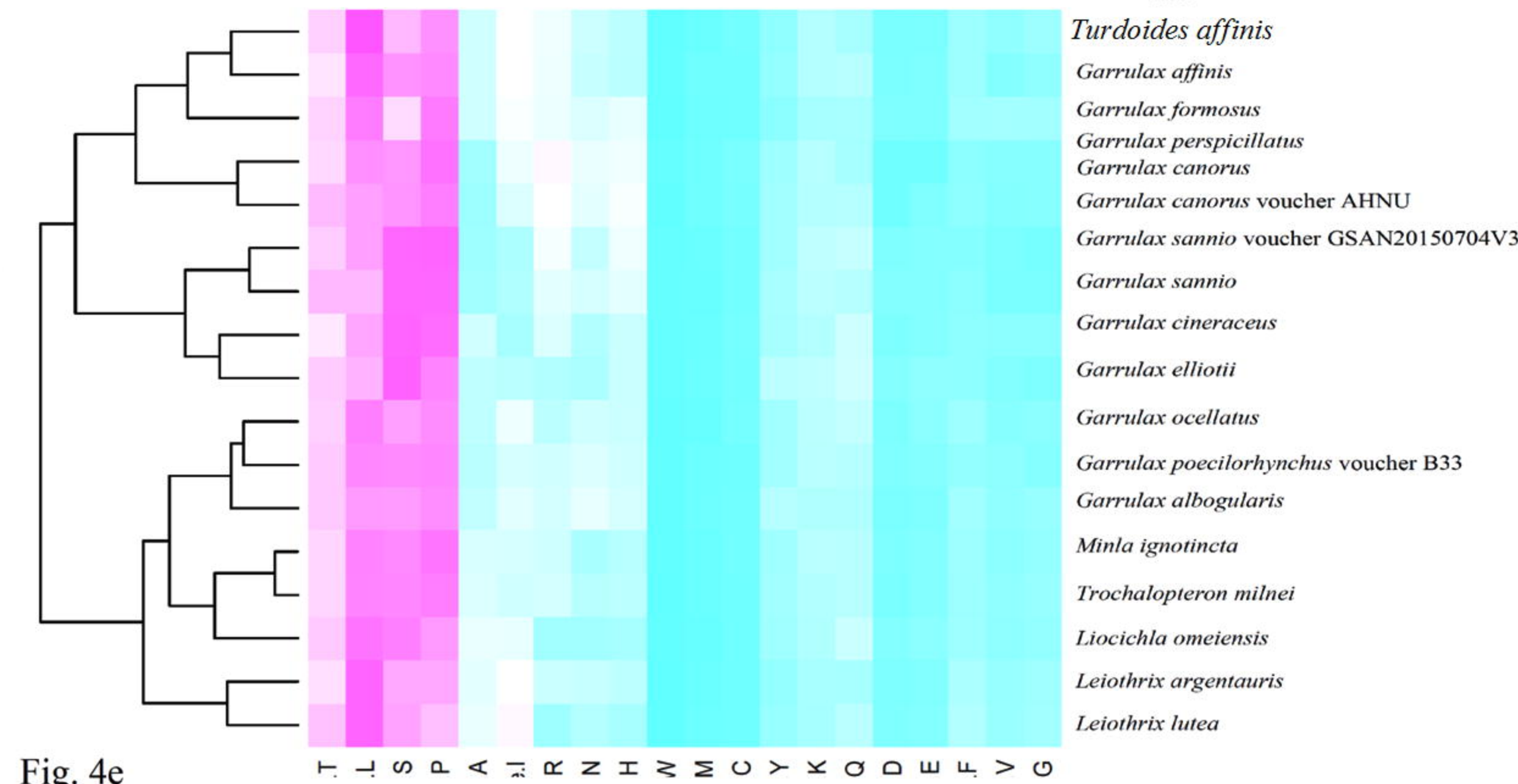


Fig. 4e

